KINETICS OF THERMAL DECOMPOSITION OF COPPER(II) ACETATE MONOHYDRATE

A. Y. Obaid, A. O. Alyoubi, A. A. Samarkandy, S. A. Al-Thabaiti, S. S. Al-Juaid, A. A. El-Bellihi[*] and El- H. M. Deifallah

Chemistry Department, Faculty of Science, King Abdulaziz University, Jeddah, P.O. Box 9028
Saudi Arabia

Abstract

The thermal decomposition of copper(II) acetate monohydrate was studied in air and nitrogen atmospheres by means of DTA-TG and SEM measurements. The kinetics of the thermal decomposition steps in air was studied by using isothermal and non-isothermal thermogravimetric techniques. The results are discussed in terms of various reaction interface models and different techniques of computational analysis of non-isothermal data. The activation parameters, calculated by using a composite method of integral analysis of non-isothermal data, revealed not only their independence from the heating rate and fractional reaction, but also a better correlation and agreement with the results obtained under isothermal conditions.

Keywords: copper acetate, decomposition, ESM, DTA, TG

Introduction

Several studies have been performed on the thermal decomposition behaviour of metal acetates [1, 5], but less information is available on the kinetics of the reactions [4, 5]. On decomposition, metal acetates often yield acetone and acetic acid, and there may be incomplete melting and some hydrolysis of hydrated salts [1]. Leicester and Redman [2] studied the thermal decompositions of nickel and cobalt acetates and found that they proceeded via an initial cleavage to metal oxide and acetic anhydride, and thence to various pyrolysis products of the anhydride. Clough *et al.* [3] suggested that the initial step in the thermal decomposition of uranyl acetate could be the fission of the UO_2–O bond, producing acetate radicals which react to give various pyrolysis products.

In the thermal decomposition of Cu(II) carboxylates, Cu^+ salts have been identified as intermediates, and the reduction of Cu(II) proceeds in two steps ($Cu^{2+} \rightarrow Cu^+ \rightarrow Cu^0$), with a possibly appreciable overlap of the consecutive rate processes [6].

---

[*]   To whom all correspondence should be addressed.

All methods of kinetic analysis of the thermal decomposition of solids yield results of a relative character, depending markedly on procedural variables [7], including the sample mass, the heating rate, the particle size and the partial pressure of the ambient atmosphere. There are a variety of computational methods and the analysis of kinetic data may not allow the choice of a single model to explain the results, which makes the establishment of a dependable correlation more difficult. However, applicable reaction models identify the chemical change occurring at the reaction interfaces, which progressively advance into the unchanged reactant [6]. The importance of characterizing the chemistry of the interface reactions and of elucidating the chemical steps through which the reactants are converted into products has been emphasized.

In the present investigation, the thermal decomposition behaviour of copper(II) acetate monohydrate has been studied by using DTA-TG and SEM techniques. The kinetics of the isothermal and non-isothermal dehydration and decomposition of copper(II) acetate monohydrate was studied in air. The composite method of kinetic integral analysis of non-isothermal data was applied to identify the mechanistic equation describing the geometry of advance of the reaction interface and to calculate the activation parameters. The results were compared with those obtained by using the isothermal technique and other integral methods of analysis of non-isothermal data.

Experimental

The copper(II) acetate monohydrate crystalline powder, a BDH product of reagent grade, was used without further purification.

Simultaneous DTA-TG experiments were performed with a Shimadzu DT 30 thermal analyser. The experiments were performed under isothermal conditions or at different specified heating rates in air at a flow rate of 3.0 l h^{-1}. The sample mass in the Pt cell of the thermal analyser was kept at about 8 mg in all experiments, in order to ensure a linear heating rate and accurate temperature measurements.

Samples of copper acetate monohydrate were inserted into an electric oven at room temperature in air and the temperature was raised to the desired value, which was maintained for 30 min before the sample was removed and cooled to room temperature in air in a desiccator. The changes taking place in morphology and texture during the thermal decomposition of the salt were investigated by using a JEOL T 300 scanning electron microscope. Samples of the parent compound and the products formed in the different stages during the decomposition were examined.

Kinetic consideration

In general, the rate constant, k of a solid-state reaction is given by the formal kinetic equation:

$$\frac{d\alpha}{dt} = kf(\alpha) = Ae^{-E/RT} f(\alpha) \tag{1}$$

where α is the fractional reaction; t, is time; A is the pre-exponential factor; E is the activation energy; R is the gas constant; T is temperature in Kelvin, and $f(\alpha)$ is the kinetic function, which takes different forms depending on the particular reaction rate equation [7–9]. In isothermal kinetic studies, the rate equation used to calculate the rate constant has the form

$$g(\alpha)=kt \tag{2}$$

where $g(\alpha)=\int_0^\alpha \dfrac{d\alpha}{f(\alpha)}$ is the integrated form of $f(\alpha)$ [7–9]. However, non-isothermal

methods are becoming more widely used because they are more convenient than the classical isothermal methods [10].

In non-isothermal kinetics, the time dependence on the left side of Eq. (1) is eliminated by using a constant heating rate $\beta=dT/dt$, so that $T=T_0+\beta$, where T_0 is the starting temperature and t is the time of heating. With the use of integral methods of analysis, Eq. (1) may be written as

$$g(\alpha)=\frac{A}{\beta}\int_{T_0}^{T}e^{-E/RT}dt \tag{3}$$

The reaction rate is negligible at low temperatures. Hence:

$$g(\alpha)=\frac{A}{\beta}\int_{0}^{T}e^{-E/RT}dt \tag{4}$$

Integration of this equation leads to Doyle's equation [11]:

$$g(\alpha)=\frac{AE}{R\beta}\left[\frac{e^{-x}}{x}-\int_0^\infty\frac{e^{-u}}{u}du\right]=\frac{AE}{R\beta}P(x) \tag{5}$$

where $u=E/RT$ and x is the corresponding value of u at which a fraction of material has decomposed. This equation has been reformulated [12] as

$$\ln g(\alpha)-\ln P(x)=\ln\frac{AE}{R\beta}=B \tag{6}$$

where B is a constant for a particular reaction at a constant heating rate β. The integral function $P(x)$ is not definite; it may be written in an expanded form and estimated by using a procedure of trial-and-error type involving iteration [13].

In the present study, analysis of non-isothermal data was performed by using the approximate computational approaches due to Coats and Redfern [14], Ozawa [15], Mahusudanan [16] and Diefallah [17]. Integral methods are often more reliable and generally preferred than differential methods of kinetic analysis.

In the Coats-Redfern method [14], the function $g(\alpha)$ is approximated to the form

$$g(\alpha)=\frac{ART^2}{\beta E}\left[1-\frac{2RT}{E}\right]e^{-E/RT} \tag{7}$$

The equation has been written in the form:

$$-\ln\left[\frac{g(\alpha)}{T^2}\right]=-\ln\frac{AR}{\beta E}\left(1-\frac{2RT}{E}\right)+\frac{E}{RT} \tag{8}$$

The quantity $\ln[(AR)/(\beta E)](1-2RT/E)$ is reasonably constant for most values of E and in the temperature range over which most reactions occur. However, both E and A could vary with the experimental heating rate.

In the Ozawa method [15], a master curve has been derived from the TG data obtained at different heating rates (β) by using Doyle's equation and assuming that $[AE/\beta R]p(E/RT)$ is a constant for a given function of material decomposed. The function $p(E/RT)$ was approximated by the equation:

$$\log p\left(\frac{E}{RT}\right)=-2.315-0.4567\left(\frac{E}{RT}\right) \tag{9}$$

so that

$$-\log\beta=0.4567\left(\frac{E}{RT}\right)+\text{constant} \tag{10}$$

Hence, the activation energy is calculated from the thermogravimetric data obtained at different heating rates. The frequency factor is calculated from the equation

$$\log A=\log g(\alpha)-\log\left[\frac{E}{\beta R}p\frac{E}{RT}\right] \tag{11}$$

Although the calculated activation energy is independent of the reaction model, and the frequency factor depends on the determined form of $g(\alpha)$, both E and A could vary considerably with the fractional reaction [7].

In the Madhusudanan method [16], the equation used has the form

$$-\ln\left[\frac{g(\alpha)}{T^{1.921503}}\right]=-\ln\frac{AR}{\beta E}+3.7720501-1.921503\ln E-\frac{E}{RT} \tag{12}$$

where the symbols have their usual significance. The activation energy E and the frequency factor A are obtained from the slope and intercept of the linear fit of the plot of $-\ln[g(\alpha)/T^{1.921503}]$ vs. $1/T$.

In the composite method of analysis of dynamic data [7], the results obtained (not only at different heating rates, but also at different α values) are superimposed on one master curve. This was achieved by rewriting the approximate integral equations due to different workers in a form such that the kinetic function $g(\alpha)$ and the linear heating rate β lie on one side of the equation and $1/T$ on the other side. When use is made of the modified Coats-Redfern equation [14], then in order to allow the composite analysis the equation is written in form

$$\ln\left[\frac{\beta g(\alpha)}{T^2}\right]=\ln\left(\frac{AR}{E}\right)-\frac{E}{RT} \tag{13}$$

Hence, the dependence of $\ln[\beta g(\alpha)/T^2]$ calculated for different α values at their respective β values on $1/T$ must give rise to a single master straight line for the correct form of $g(\alpha)$, and a single activation energy and frequency factor can readily be calculated.

When Doyle's approximate equation [11] is used, the equation for composite analysis has the form

$$\log[\beta g(\alpha)]=\left[\log\frac{AE}{R}-2315\right]-0.4567\frac{E}{RT} \qquad (14)$$

Use may also be made of the approximate equation [16] of Madhusudanan, rewritten as

$$-\ln\left[\frac{\beta g(\alpha)}{T^{1.921503}}\right]=-\ln\frac{AR}{E}+3.7720501-1.9211503\ln E-\frac{E}{RT} \qquad (15)$$

Again, the dependence of the left side of Eqs (14) and (15) on $1/T$ should give rise to a single master straight line for the correct form of $g(\alpha)$, and hence the activation energy and the frequency factor can readily be calculated.

In general, the use of the different approximate integral equations for the kinetic analysis of non-isothermal decomposition kinetic data according to the composite method of analysis gave rise, within experimental error, to identical values of the activation parameters and the correct form of $g(\alpha)$. A computer program has been written to perform the data analysis [17].
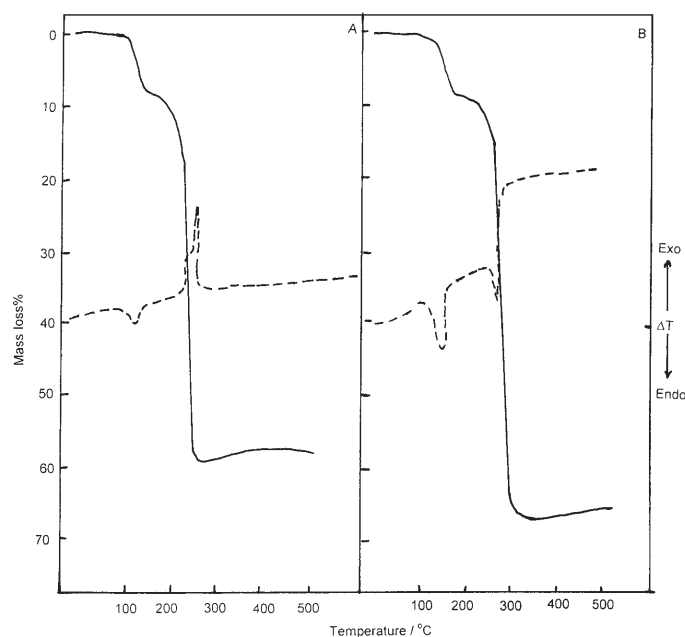

Fig. 1 DTA-TG curves for copper(II) acetate monohydrate in A – air and B – nitrogen at a heating rate of 15°C min^{-1}

Results and discussion

Figure 1 shows the DTA-TG curves obtained for $Cu(CH_3COO)_2 \cdot H_2O$ in air (*A*) and nitrogen (*B*), respectively. The TG curve contained two steps due to dehydration and decomposition of the anhydrous salt, in general agreement with previous studies [4]. The first step was endothermic and took place in the temperature range 110–150°C, involving the loss of one molecule of water with a mass loss of about 10%. The second step started at about 200°C and was complete by about 300°C; it was endothermic in nitrogen, and exothermic in air, due to oxidation. It corresponded to a mass loss of about 58%, due to decomposition of the anhydrous salt to copper metal. In air, above 300°C, a slight mass increase was observed in the TG curve and a corresponding broad exothermic peak in the DTA curve, due to the partial oxidation of Cu to CuO.

    SEM micrographs indicating the changes in morphology and texture that accompany the salt decomposition are shown in Fig. 2. Each sample was calcined for
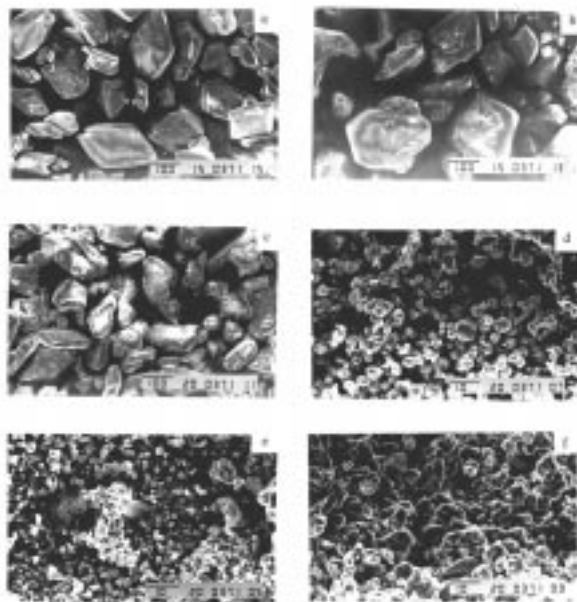

Fig. 2 Scanning electron micrographs showing the changes in texture and morphology that accompany the thermal decomposition of copper(II) acetate monohydrate in air: a – parent compound at room temperature, displaying relatively large crystals of different sizes; b – parent compound after partial dehydration at 120°C; c – sample calcined at 200°C after complete dehydration of the parent compound to the anhydrous salt; d – sample calcined at 300°C, showing partial decomposition and fissioning of the anhydrous salt; e – sample calcined at 500°C, showing complete decomposition of the anhydrous salt into small crystallites with a cubic crystal habit and some aggregation of particles; f – sample calcined at 800°C, showing coalescence of the small crystallites into large aggregates accompanying the oxidation of Cu to CuO; (scale bar: a, b and c – 100 µm; d, e and f – 10 µm)

about 30 min at the specified temperature. The results reveal that the particle shape and size change throughout the decomposition. The regular shape of the parent reactant crystallites (Fig. 2(a)), underwent some superficial roughening, after partial dehydration at 120°C, (Fig. 2(b)), whereas complete dehydration at 200°C resulted in more roughening and cracking of the crystallite surface (Fig. 2(c)). At 300°C, the an-

Table 1 Activation parameters of the thermal dehydration and decomposition of $Cu(CH_3COO)_2 \cdot H_2O$, calculated according to the R_2 model

Method of analysis		Dehydration step		Decomposition step	
		E/kJ mol^{-1}	$\lg A$/min^{-1}	E/kJ mol^{-1}	$\lg A$/min^{-1}
Isothermal		107.8±4.3	13.1±0.5	71.2±3.7	6.0±0.3
Non-isothermal					
	β				
	2	180.3	23.0	92.7	8.2
	5	129.3	16.0	95.0	8.4
a) Coats-Redfern	10	118.5	14.6	95.9	8.6
	15	118.8	13.7	106.0	9.7
	20	87.8	10.7	117.7	10.3
	Average	125.5±23.4	15.6±3.1	100.3±6.9	9.0±0.8
	β				
	2	180.6	23.0	93.1	8.2
	5	134.8	16.8	95.3	8.5
b) Madhusudanan	10	118.8	14.6	96.2	8.6
	15	112.0	13.7	106.3	9.7
	20	88.0	10.6	112.0	10.3
	Average	126.8±24.7	15.7±3.3	100.6±6.9	9.1±0.8
	1−α				
	0.1	182.7	23.8	92.3	8.2
	0.2	145.8	18.5	93.7	8.3
	0.3	129.7	16.2	98.7	8.9
	0.4	123.2	15.3	107.9	9.9
c) Ozawa	0.5	115.7	14.3	117.2	10.9
	0.6	112.0	13.7	124.5	11.7
	0.7	105.7	12.9	129.6	12.2
	0.8	99.2	12.0	142.0	13.5
	0.9	88.9	10.6	148.0	14.2
	Average	122.5±20.2	15.3±2.8	117.1±16.8	10.9±1.8
d) Composite		117.7±4.2	14.5±1.3	100.2±1.9	9.1±0.5

hydrous salt, after partial decomposition, had undergone extensive degradation with a reduction in particle size from more than about 100 µm to less than about 4 µm. At 500°C, after complete decomposition of the anhydrous salt to Cu° metal, the particle size was further reduced to less than about 2 µm, with a cubic crystal habit. At 800°C, the small crystallites coalesced into aggregates of irregular shape and size, accompanying the oxidation of copper to Cu(II) oxide.

Figure 3 shows plots of isothermal fractional reaction *vs.* time curves, whereas Fig. 4 depicts the fractional reaction remaining as a function of temperature, for the dehydration and decomposition steps. The curves in Fig. 3 exhibited a deceleratory
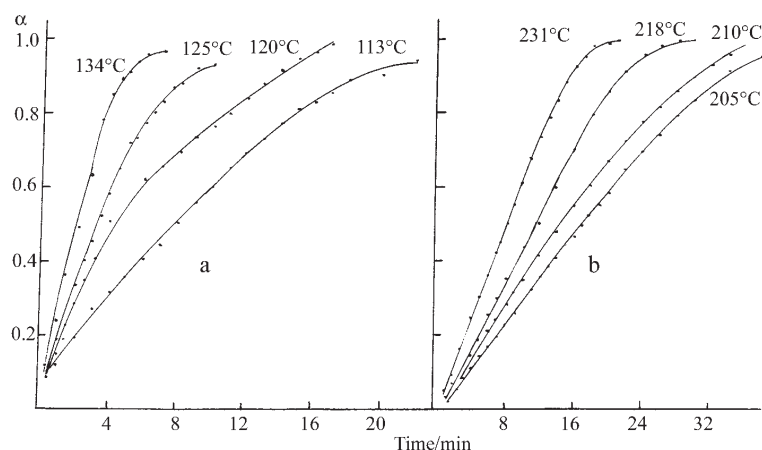

Fig. 3 Isothermal α/t curves for the decomposition of copper(II) acetate monohydrate in air: a – dehydration step; b – decomposition step
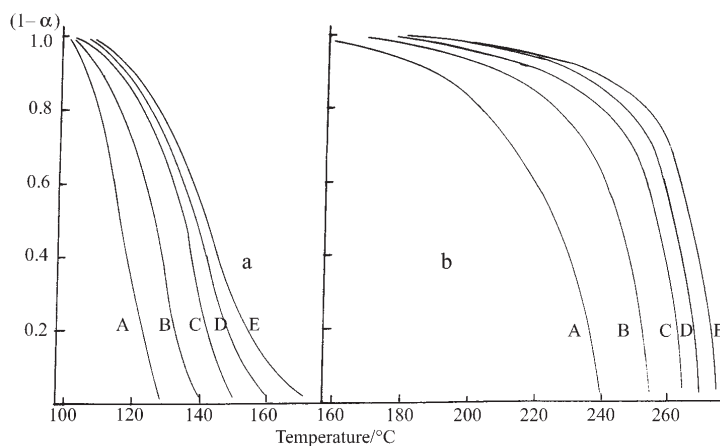

Fig. 4 Dynamic measurements for the thermal decomposition of copper(II) acetate monohydrate in air: a – dehydration step; b – decomposition step. Heating rate: curve A – 2°C min^{-1}; curve B – 5°C min^{-1}; curve C – 10°C min^{-1}; curve D – 15°C min^{-1} and curve E – 20°C min^{-1}
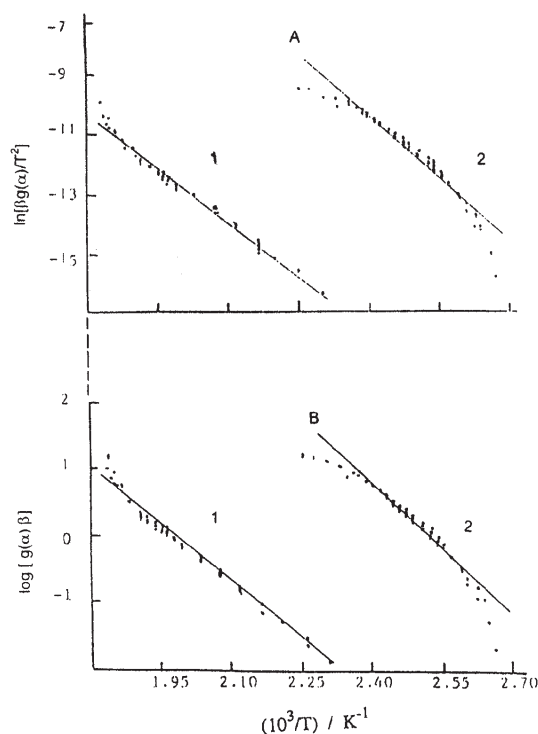
Fig. 5 Composite analysis of the dynamic TG data based on the modified
Coats-Redfern equation (A) and Doyle's equation (B), assuming the contracting
surface (R_2) model. 1 – dehydration step; 2 – decomposition step

shape, and kinetic analyses of the two steps were performed with reference to the different models of heterogeneous solid-state reactions [7–9]. The method of least square regression analysis was performed for each of the tested functions, and it was found that the two-dimensional phase boundary and the first-order reaction models gave the best fits for both the dehydration and the decomposition steps. Analyses of the non-isothermal data were performed according to the integral methods of Coats-Redfern, Ozawa, Madhusudanan and Diefallah, and the activation parameters were calculated. They are listed in Table 1, in comparison with those obtained from the analysis of the isothermal data.

Figure 5 shows typical composite plots for the dehydration and decomposition steps according to the contracting surface (R_2) equation, which gives better regression factors and standard deviations than those for the other models.

The results in Table 1 demonstrate that the integral composite analysis of the dynamic data gave better agreement with the isothermal results, with a higher correlation and less deviation in the calculated experimental parameters. The activation energy for the dehydration step is in agreement with that reported by Mu and Perlmutter [5] and indicates that the water of hydration is co-ordinated water. The activation en-

ergy for the decomposition of the anhydrous salt is lower than the values of many thermal decomposition reactions, which may indicate the catalytic action of the fine-grained copper metal particles formed in the early stages of the decomposition step. This supports the view that charge transfer is the rate-controlling step in the mechanism of carboxylate decompositions [1].

<p style="text-align:center">* * *</p>

References

1 A. K. Galwey, in MTP International Review of Science, Inorganic Chemistry, Series 2, Solid State Chemistry, Vol. 10, H. J. Emeleus (ed.), Butterworths, London 1975, p. 147.

2 J. Leicester and M. H. Redman, J. Appl. Chem., 12 (1962) 357.

3 P. S. Clough, D. Dollimore and P. Grundy, J. Inorg. Nucl. Chem., (1969) 361.

4 A. Afzal, P. K. Butt and A. Ahmad, J. Thermal Anal., 37 (1991) 1015.

5 J. Mu and D. D. Perlmutter, Thermochim. Acta, 49 (1981) 207.

6 A. K. Galwey, J. Thermal Anal., 41 (1994) 267.

7 El-H. M. Diefallah, Thermochim. Acta, 202 (1992) 1.

8 M. E. Brown, D. Dollimore and A. K. Galwey, Comprehensive Chemical Kinetics, Vol. 22, Elsevier, Amsterdam 1980.

9 M. E. Brown, Introduction to Thermal Analysis, Chapman and Hall, 1988, Chapter 13.

10 D. Chen, X. Gao and D. Dollimore, Analytical Instrumentation, 20 (1992) 137.

11 C. D. Doyle, Nature, 207 (1965) 290.

12 J. Zsakó, J. Thermal Anal., 2 (1970) 145.

13 B. Carrol and E. P. Manche, Thermochim. Acta, 3 (1972) 449.

14 A. W. Coats and J. P. Redfern, Nature, 201 (1964) 68.

15 T. Ozawa, Bull. Chem. Soc. Jpn., 38 (1965) 1881; J. Thermal Anal., 2 (1970) 301.

16 P. M. Madhusudanan, Thermochim .Acta, 97 (1986) 189.

17 El-H. M. Diefallah, A. Y. Obaid, A. H. Qusti, A. A. El-Bellihi and M. Abdel Wahab, Thermochim. Acta, 274 (1996) 172.